On the Numerical Approximation and Computation of Minimal-Surface-Continua bounded by One-Parameter-Families of Polygonal Contours

Michael Hinze
Fachbereich Mathematik
Technische Universität Berlin

Abstract

Minimal surfaces bounded by a polygon $\Gamma \subset \mathbb{R}^q (q \geq 2)$ correspond in a one-to-one mannner to the critical points of Shiffman's function Θ. For arbitrary, but fixed polygons this function was investigated numerically in [16]. The present work extends the results in [16] to classes of polygons $\Gamma = \Gamma(\alpha)$, where α varies in certain subsets of finite dimensional spaces the dimensions of depending on the number of vertices of the polygon Γ. In the numerical part investigations on the bifurcation process of one-parameter families of polygonal approximations of three well-known contour families are presented.

1 Introduction

Let Γ be a Jordan curve in $\mathbb{R}^q$ $(q \geq 2)$ and denote by $B = \{w = (x_1, x_2) \in \mathbb{R}^2;\ |w| < 1\}$ the unit disc in $\mathbb{R}^2$. A mapping $u \in C^0(\overline{B}, \mathbb{R}^q) \cap C^2(B, \mathbb{R}^q)$ is called disc type minimal surface spanning Γ if u satisfies

$$\Delta u = 0 \quad \text{in } B \tag{1}$$

$$|u_{x_1}|^2 - |u_{x_2}|^2 = (u_{x_1}, u_{x_2}) = 0 \quad \text{in } B \tag{2}$$

$$u_{|_{\partial B}} \quad \text{is a (weakly) monotone parametrization of } \Gamma. \tag{3}$$

In the case where Γ is a simple, closed polygon, the minimal surface problem is connected with the critical points of a function of finitely many variables. To be more precise, let $\alpha = (a_1, \ldots, a_{N+3})$ denote the distinct vertices of the polygon $\Gamma = \Gamma(\alpha)$ $(N \geq 1)$ and consider mappings $v : \overline{B} \to \mathbb{R}^q$ in $C^0(\overline{B}, \mathbb{R}^q) \cap C^1(B, \mathbb{R}^q)$ such that $v(-1) = a_{N+1}$, $v(-i) = a_{N+2}$, $v(1) = a_{N+3}$ and $v(e^{i\kappa_j}) = a_j$ $(1 \leq j \leq N)$, where $\kappa = (\kappa_1, \ldots, \kappa_N)$ is an N-tuple of parameter values κ_j satisfying $0 < \kappa_1 < \ldots < \kappa_N < \pi$. Let $F'(\kappa, \alpha)$ denote the classes of such mappings which map the arc $\overline{\gamma}_j := \{e^{i\phi}; \kappa_j \leq \phi \leq \kappa_{j+1}\}$ in a weakly monotone way onto the segment $[a_j, a_{j+1}]$ on the straight line $a_j + \Gamma_j(\alpha)$ through the points a_j, a_{j+1} $(\kappa_j \equiv \kappa_l \ if\ j \equiv l \ mod\ N+3)$ $(1 \leq j \leq N+2)$. Disc-type minimal surfaces spanning $\Gamma(\alpha)$ now correspond in a one-to-one manner to the critical points of Courant's function

$$d(\kappa, \alpha) := \inf_{v \in F'(\kappa, \alpha)} D(v), \tag{4}$$

where Dirichlet's integral is defined by

$$D(v) := \frac{1}{2} \int_B |\nabla v|^2 dx. \tag{5}$$

Problem (4) has a unique solution $v(\kappa,\alpha)$, called *minimal vector* (see [3, Lemma 6.3]). The function d is known to be of class C^1. Unfortunately, it is not known up to now whether d is of class C^2, therefore Courant's function is not a good candidate to develop a Morse theory for polygonal minimal surfaces.

The Marx-Shiffman function Θ was introduced in the paper of Marx [20], which was based on a joint work of Marx and Shiffman concerning polygonally bounded minimal surfaces. Marx and Shiffman enlarged the classes $F'(\kappa,\alpha)$ to the class $F(\kappa,\alpha)$ of mappings which map the arc γ_j into the straight lines $a_j+\Gamma_j(\alpha)$ and defined

$$\Theta(\kappa,\alpha) := \inf_{v\in F(\kappa,\alpha)} D(v). \tag{6}$$

The unique solution $u(\kappa,\alpha)$ of problem (6) is called *(normalized) quasiminimal surface*. As a result, we clearly have $d(\kappa,\alpha)\geq\Theta(\kappa,\alpha)$ and $d(\kappa,\alpha)>\Theta(\kappa,\alpha)$ for certain values of κ (see [19]). In [20], it was stated that Θ is of class C^∞. In [8], [10] Heinz proved that the quasiminimal surfaces $u(\kappa,\alpha)$ depend analytically on κ,α. Using this result Heinz was able to prove that Θ is analytic ([9], [10]). Furthermore, according to Heinz the critical points of Θ correspond in a one-to-one manner to solutions of a generalized Plateau problem for $\Gamma(\alpha)$. Here, *generalized* means : the solution $u(\kappa,\alpha)$ can overshoot the vertices and we only know that $u(\gamma_j,\alpha)\subset a_j+\Gamma_j(\alpha)$. Note, that d and Θ are closely connected as they coincide at the critical points of d (see [27]).

In the last years several numerical approaches to the boundary value problem for parametric minimal surfaces had been made. Here, we mention the works of Jarausch [18], Wohlrab [32], Tsuchija [29], [30],[31], Dziuk [6], Hutchinson [17], Pinkall/Polthier [23], Dziuk/Hutchinson [7], the author [13], [14], [15], [16] and refer to the references therein.

In this work the numerical results presented in [15], [16] are extended to one-parameter families of polygonal contours. The method is based on the numerical treatment of Θ and a suitable approximation of $\nabla\Theta$. Using piecewise linear finite elements, discrete quasiminimal surfaces $u_h(\kappa,\alpha)$ are computed. This yields an approximation $\Theta_h(\kappa,\alpha)=D_h(u_h(\kappa,\alpha))$ of Θ. Based on an explicit expression for $\nabla\Theta$, that only involves the quasiminimal surface $u(\kappa,\alpha)$ a discrete approximation f_h of $\nabla\Theta$ is introduced. Newton's method applied to the equation $f_h(\kappa,\alpha)=0$ then gives approximations of critical points of Θ. The corresponding quasiminimal surfaces are approximations of generalized minimal surfaces bounded by $\Gamma(\alpha)$. In a next step, for α varying in a one-parameter family of values numerical pathfollowing can be applied to the equation $f_h(\kappa,\alpha)=0$. Of particular interest are contour families where the solution behaviour of the Plateau-Problem for $\Gamma(\alpha)$ changes at some parameter value α. In this case numerical pathfollowing provides a tool for investigating the bifurcation process at such critical parameter values numerically. As an illustration the bifurcation process for three well known contour families is investigated numerically. This is the first time that numerical pathfollowing is applied to computing approximations of minimal surfaces.

For the visualization of grids and discrete surfaces the the graphical programing environment GRAPE developed at the Sonderforschungsbereich 256 at the university of Bonn, Germany is used. The computation of the bifurcation diagrams is performed by using the ALCON2-program developed at the Konrad-Zuse-Zentrum, Berlin for the purpose of computing solution sets of parameter dependant equations.

2 Notations and analytical preliminaries

In what follows, N and q denote integers with $N\geq 1$ and $q\geq 2$. Let $B:=\{w=x_1+ix_2;|w|<1\}\subset\mathbb{C}\quad\equiv\{\mathrm{x}=(\mathrm{x}_1,\mathrm{x}_2);|\mathrm{x}|<1\}\subset\mathbb{R}^2$ denote the unit disc and let $\Gamma\subset\mathbb{R}^q$ be a closed polygon with $N+3$ distinct

vertices $a_1, \ldots, a_{N+3}$ arranged in cyclical order. To Γ assign a unique point

$$\alpha \;=\; (a_1^1, \ldots, a_1^q, \ldots, a_{N+3}^1, \ldots, a_{N+3}^q) \in \mathbb{R}^{q(N+3)} \tag{7}$$

and write $\Gamma = \Gamma(\alpha)$. Set

$$\varphi_k(\alpha) := \frac{a_{k+1} - a_k}{|a_{k+1} - a_k|} \quad (1 \le k \le N+3; a_{N+4} := a_1) \tag{8}$$

and

$$\tilde{A} \;:=\; \{\alpha \in \mathbb{R}^{q(N+3)};\ \varphi_k, \varphi_{k+1} \text{ are linearly independent for } k = 1, \ldots, N+2\}. \tag{9}$$

For $\alpha \in \tilde{A}$ and $k = 1, \ldots, N+3$, $\Gamma_k(\alpha)$ denotes the line

$$\Gamma_k(\alpha) \;=\; \{x \in \mathbb{R}^q; x = t\varphi_k(\alpha), t \in \mathbb{R}\} \tag{10}$$

and $S_k(\alpha)$, $T_k(\alpha)$ denote the reflections at the lines $\Gamma_k(\alpha)$ and $a_k + \Gamma_k(\alpha)$, respectively. Let $\kappa = (\kappa_1, \ldots, \kappa_N) \in \mathbb{R}^N$ denote an $N-tuple$ of parameter values κ_j satisfying

$$0 < \kappa_1 < \ldots < \kappa_N < \pi \tag{11}$$

and define

$$T \;:= \{\kappa \in \mathbb{R}^N;\ 0 < \kappa_1 < \ldots < \kappa_N < \pi\}. \tag{12}$$

In order to connect the problem (6) with the Plateau problem for the polygon Γ let

$$\kappa_{N+1} := \pi, \quad \kappa_{N+2} := \frac{3\pi}{2}, \quad \kappa_{N+3} := 2\pi. \tag{13}$$

$T' \subset\subset T$ always denotes a compact subset of T. For $\kappa \in T$ define

$$\gamma_k(\kappa) := \{w = e^{i\phi}; \kappa_k < \phi < \kappa_{k+1}\} \quad (1 \le k \le N+3;\ \kappa_{N+4} \equiv \kappa_1 + 2\pi) \tag{14}$$

and abbreviate

$$\beta_k(\kappa) := e^{i\kappa_k} \quad (1 \le k \le N+3). \tag{15}$$

The convention is used that dependencies on fixed parameter values are not explicitly stated, i.e. one writes X instead of $X(\kappa, \alpha)$ if κ and α are fixed, $X(\kappa)$ instead of $X(\kappa, \alpha)$ if only α is fixed and $X(\alpha)$ if only κ is fixed.

For $m \in \mathbb{N}_0$ and $1 \le p \le \infty$, $H^{m,p}(\Omega)$ denotes the Sobolev space of all Lebesgue-measurable functions having p-integrable derivatives up to order m equipped with the usual norm $\|\cdot\|_{m,p,\Omega}$. The corresponding seminorms are denoted by $|\cdot|_{m,p,\Omega}$. Abbreviate $H^m(\Omega) \equiv H^{m,2}(\Omega)$, $\|f\|_{m,\Omega} \equiv \|f\|_{m,2,\Omega}$, $|f|_{m,\Omega} \equiv |f|_{m,2,\Omega}$ as well as $\|f\|_\Omega \equiv \|f\|_{0,\Omega}$.

For $k \in \mathbb{N}_0$, $C^k(\Omega)$ denotes the space of all functions having continuous derivatives up to order k. Denote by $C^k(\overline{\Omega})$ the set of all functions in $C^k(\Omega)$, such that, for $|s| \le k$, there exists a continuous extension of $\partial^s f$ onto $\overline{\Omega}$.

$H^{m,p}(\Omega, \mathbb{R}^q)$ is defined as the set of all vector-valued functions $f = (f_1, \ldots, f_q)$, such that $f_i \in H^{m,p}(\Omega)$ $(1 \le i \le q)$. The function spaces $C^k(\Omega, \mathbb{R}^q)$ and $C^k(\overline{\Omega}, \mathbb{R}^q)$ are defined analogously.

Introducing the function spaces

$$X(\kappa,\alpha) \;:=\; \{v \in H^1(B,\mathbb{R}^q);\; v(\gamma_k(\kappa)) \subset a_k + \Gamma_k(\alpha)\;\; (1 \le k \le N+3)\} \tag{16}$$

and

$$X_0(\kappa,\alpha) := \{v \in H^1(B,\mathbb{R}^q)\;;\; v(\gamma_k) \subset \Gamma_k(\alpha) \quad (1 \le k \le N+3)\}. \tag{17}$$

problem (6) according to [14, Theorem 3.1] alternatively can be written as

$$\Theta(\kappa,\alpha) = \inf_{v \in X(\kappa,\alpha)} D(v) \qquad (\kappa \in T). \tag{18}$$

This problem has a unique solution $u = u(\kappa,\alpha) \in C^0(\overline{B},\mathbb{R}^q) \cap C^2(\overline{B} \setminus \{\beta_1,\ldots,\beta_{N+3}\},\mathbb{R}^q)$ that satisfies

$$\int_B \nabla u\, \nabla v\, dx \;=\; 0 \qquad \forall\; v \in X_0 \tag{19}$$

and solves the following system of partial differential equations (see [8, Satz 1])

$$\Delta u \;=\; 0 \qquad in\; B \tag{20}$$

$$u(\gamma_k) \;\subset\; a_k + \Gamma_k \qquad 1 \le k \le N+3 \tag{21}$$

$$(\partial_r u, \varphi_k) \;=\; 0 \qquad on \quad \gamma_k, \quad 1 \le k \le N+3. \tag{22}$$

Since u is continuous on $\overline{B}$ by necessity there holds

$$u(\beta_k) = a_k \quad (k = 1,\ldots,N+3).$$

At the vertices of Γ the normal to the contour has a jump discontinuity. This causes a lack of regularity of u at β_k. Heinz completely investigated this situation in [8, Satz 2], [10]. In order to formulate the corresponding theorem introduce some notations. Let $\kappa^* \in T, \alpha^* \in A$ be arbitrary, but fixed. For $\epsilon > 0$, $(\kappa,\alpha,w) \in \mathbb{C}^{\mathrm{N}} \times \mathbb{C}^{\mathrm{q(N+3)}} \times \mathbb{C}$ set

$$U_\epsilon(\kappa^*,\alpha^*,\beta_k(\kappa^*)) := \{(\kappa,\alpha,w); |(\kappa,\alpha,w) - (\kappa^*,\alpha^*,\beta_k(\kappa^*))| < \epsilon\} \quad (1 \le k \le N+3). \tag{23}$$

In what follows assume that

H: *For every* $\alpha \in \tilde{A}$, $\Gamma(\alpha)$ *has an angle different from* $90°$ and $q \le 3$

and define

$$A \;:=\; \{\alpha \in \tilde{A}; \Gamma(\alpha) \text{ satisfies } \mathtt{H}\}. \tag{24}$$

From [10, Satz 1, Satz 3] one obtains the following theorem.

Theorem 2.1 *Let* $D = D(\kappa^*) \subset \mathbb{C}$ *denote a simply connected region, such that* $D \cap B$ *is nonempty, connected and the closure* $\overline{D}$ *does not contain any of the points* $\beta_j(\kappa^*)$ $(j = 1,\ldots,N+3)$. *Then, there exist polydiscs*

$$U_D(\kappa^*) = \{\kappa \in \mathbb{C}^{\mathrm{N}}; |\kappa_{\mathrm{j}} - \kappa_{\mathrm{j}}^*| < \epsilon_{\mathrm{D}},\; \mathrm{j} = 1,\ldots,\mathrm{N}\},$$

$$U(\alpha^*) = \{\alpha \in \mathbb{C}^{\mathrm{q(N+3)}}; |\alpha_{\mathrm{l}} - \alpha_{\mathrm{l}}^*| < \hat{\epsilon}\}$$

and a function $f_D(\kappa,\alpha,w)$, *which is analytic in* $U_D(\kappa^*) \times U(\alpha^*) \times D$, *such that for the solutions* $u(\kappa,\alpha)(w)$ *of (18) one has*

$$u_w(\kappa,\alpha)(w) = f_D(\kappa,\alpha,w) \quad \forall\; (\kappa,\alpha,w) \in (U_D(\kappa^*) \cap T) \times (U(\alpha^*) \cap A') \times (D \cap B).$$

Furthermore, for every $k = 1, \ldots, N+3$ *there exists an integer* $1 \le p_k \le q$ *and an* $\epsilon_0 > 0$ *such that* $u(\kappa,\alpha)(w)$ *satisfies the singular expansions*

$$u_w(\kappa,\alpha)(w) = \sum_{j=1}^{p_k} f_j^k(\kappa,\alpha,w)(w-\beta_k(\kappa))^{p_j^k(\alpha)} \quad \forall (\kappa,\alpha,w) \in U_\epsilon(\kappa^*,\alpha^*,\beta_k(\kappa^*)) \cap (T \times A' \times B). \tag{25}$$

The complex-valued coefficient functions $f_j^k(\kappa,\alpha,w)$ *and exponent functions* $p_j^k(\alpha)$ *are analytic in* $U_{\epsilon_0}(\kappa^*,\alpha^*,\beta_k(\kappa^*))$ *and* $U(\alpha^*)$*, respectively. In* $U(\alpha^*) \cap A'$ *the relation*

$$-1 < p_1^k(\alpha) < \ldots < p_{p_k}^k(\alpha) \le 0 \quad (1 \le k \le N+3)$$

is valid. The function Θ *is analytic in* $T \times A$*.*

Integration of (25) yields for some suitable $\tilde{\epsilon}_0 > 0$ and $\forall (\kappa,\alpha,w) \in U_{\tilde{\epsilon}_0}(\kappa^*,\alpha^*,\beta_k(\kappa^*)) \cap (A \times T \times B)$

$$u(\kappa,\alpha)(w) = a_k + Re(\sum_{j=1}^{p_k} g_j^k(\kappa,\alpha,w)\ (w-\beta_k(\kappa))^{p_j^k(\alpha)+1}) \tag{26}$$

with suitable coefficient functions $g_j^k(\kappa,\alpha,w)$. The exponents $p_j^k(\alpha)$ are directly related to the eigenvalues of $S_{k-1}(\alpha)S_k^{-1}(\alpha)$ and therefore to the angles of the polygon $\Gamma(\alpha)$ at a_k $(1 \le k \le N+3)$ (see [8, (3.26),(3.28),(3.49),(3.63)]). In the case $q = 3$ one has from [10, (4.2)]

$$p_3^k = 0, \quad p_2^k = -\alpha_k, \quad p_1^k = \alpha_k - 1 \qquad (1 \le k \le N+3), \tag{27}$$

where

$$\cos \alpha_k \pi := \varphi_{k-1}^t \varphi_k \quad (k = 2, \ldots, N+3). \tag{28}$$

Using the exponents of Theorem 2.1 set for $\alpha \in A$

$$p_{min}(\alpha) := \min_{1 \le k \le N+3} \min_{1 \le j \le p_k} p_j^k(\alpha) \in (-1, 0]. \tag{29}$$

Theorem 2.1 then implies for a suitable $\tilde{\epsilon} > 0$ (compare also [11, (2.1)])

$$|u_w(\kappa,\alpha)(w)| \le\ c\ \sum_{k=1}^{N+3} |w-\beta_k(\kappa)|^{p_{min}(\alpha)} \quad (|w| < 1; |i(\kappa-\kappa^*,\alpha-\alpha^*)| < \tilde{\epsilon}) \tag{30}$$

and

$$|u_{ww}(\kappa,\alpha)(w)| \le\ c\ \sum_{k=1}^{N+3} |w-\beta_k(\kappa)|^{p_{min}(\alpha)-1} \quad (|w| < 1; |(\kappa-\kappa^*,\alpha-\alpha^*)| < \tilde{\epsilon}), \tag{31}$$

with some $c > 0$.

Next, define for $\epsilon > 0$

$$\Omega_\epsilon(\kappa) := \overline{B} \setminus \cup_{k=1}^{N+3}\ B_\epsilon(\beta_k(\kappa)), \quad \kappa \in T \tag{32}$$

and assign to every $\kappa \in T$ a simply connected domain $D(\kappa)$ in such a way, that Theorem 2.1 is valid for $\kappa = \kappa^*$. Let $T' \subset\subset T, A' \subset\subset A$ and apply Theorem 2.1 for every $(\kappa,\alpha) \in T' \times A'$ together with suitable domains $D(\kappa)$. Then the corresponding polydiscs in Theorem 2.1 induce an open covering of $T' \times A'$. Thus, the Heine-Borel theorem together with (30) and (31) proves

Corollary 2.1 *For every* $T' \subset\subset T, A' \subset\subset A$ *there exist positive constants* $c_1(T',A')$*,* $c_2(T',A',\epsilon)$*,* $c_3(T',A')$ *and some* $p_{min} = p_{min}(A') > 0$ *such that*

$$\|u(\kappa,\alpha)\|_{1,p,B}\ \le c_1(T',A') \qquad \forall\ (\kappa,\alpha) \in T' \times A'\ \forall\ 2 \le p < \frac{-2}{p_{min}}, \tag{33}$$

$$\|u(\kappa,\alpha)\|_{2,\Omega_\epsilon(\kappa)} \le c_2(T',A',\epsilon) \qquad \forall\ (\kappa,\alpha)\in T'\times A'\ \forall\ \epsilon>0,\ \Omega_\epsilon(\kappa)\neq\emptyset \tag{34}$$

and

$$|u_{ww}(\kappa,\alpha)(w)| \le c_3(T',A')\ \sum_{k=1}^{N+3} |w-\beta_k(\kappa)|^{p_{min}(\alpha)-1} \qquad \forall\ (\kappa,\alpha)\in T'\times A' \quad (|w|<1). \tag{35}$$

In particular for every $T' \subset\subset T$, there exists some $\epsilon(T')>0$ so that the assertion in the second part of Theorem 2.1 is valid for every $\kappa=\kappa^*\in T'$ and $\epsilon_0=\epsilon(T')$. For $\epsilon(T')$ inequality (34) reads

$$\|u(\kappa,\alpha)\|_{2,\Omega_{\epsilon(T')}(\kappa)} \le c_2(T',A') \qquad \forall\ (\kappa,\alpha)\in T'\times A'.$$

This Corollary is an important tool in proving a uniform error estimate for discrete quasiminimal surfaces (see Sect. 3, (46)).

In [15, Theorem 3.3.3] the following expression for the partial derivatives of Θ with respect to κ_j $(j=1,\dots,N+3)$ is computed.

$$\begin{aligned}\Theta_{\kappa_j}(\kappa,\alpha) = -\frac{1}{2}\Big\{ &\frac{1}{\kappa_{j+1}-\kappa_j}\int\limits_{S(\kappa_j,\kappa_{j+1})} (u_{x_1}^2(\kappa,\alpha)-u_{x_2}^2(\kappa,\alpha))a(x)+4u_{x_1}(\kappa,\alpha)u_{x_2}(\kappa,\alpha)b(x)dx_1dx_2 - \\ &\frac{1}{\kappa_j-\kappa_{j-1}}\int\limits_{S(\kappa_{j-1},\kappa_j)} (u_{x_1}^2(\kappa,\alpha)-u_{x_2}^2(\kappa,\alpha))a(x)+4u_{x_1}(\kappa,\alpha)u_{x_2}(\kappa,\alpha)b(x)dx_1dx_2\Big\},\end{aligned} \tag{36}$$

where $S(\kappa_{j-1},\kappa_j)$ denotes the sector of B defined by the points $0,\beta_{j-1},\beta_j$ $(j=2,\dots,N+3)$ and

$$a(x)=\frac{x_1^2-x_2^2}{x_1^2+x_2^2}, \quad b(x)=\frac{x_1x_2}{x_1^2+x_2^2} \quad x\in\overline{B}\setminus\{0\}.$$

Remark 2.1 *The previous statements remain valid for the more general function*

$$\Upsilon(\kappa,\alpha) := \inf_{v\in X(\kappa,\alpha)} D(v) \quad (\kappa\in Q,\ \alpha\in A), \tag{37}$$

where the set $Q\subset\mathbb{R}^{N+3}$ is defined by

$$Q := \{\kappa=(\kappa_1,\dots,\kappa_N+3)\in\mathbb{R}^{N+3};\ \kappa_1<\dots<\kappa_{N+3}<\kappa_1+2\pi\}$$

(see [8], [10]).
For $\kappa\in Q,\ \alpha\in A$ the unique vector function $u(\kappa,\alpha)\in X(\kappa,\alpha)$ satisfying

$$\Upsilon(\kappa,\alpha)=D(u(\kappa,\alpha))$$

is called quasiminimal surface. For $\kappa\in T$ the definition of the function $\Upsilon(\kappa,\alpha)$ now implies

$$\Theta(\kappa,\alpha)=\Upsilon(\kappa,\pi,\frac{3}{2}\pi,2\pi,\alpha) \quad (\kappa\in T,\ \alpha\in A).$$

The next Theorem was proved by Heinz in [9, Satz] and characterizes minimal surfaces in terms of Θ.

Theorem 2.2 *For $\kappa\in T$ the surface $u(\kappa)$ is a minimal surface iff $\nabla\Theta(\kappa)=0$.*

Consequently, Plateau's problem for Γ is analytically embedded into a N-parameter family of quasiminimal surfaces.

Due to results of Heinz ([12, Satz 2]) and Sauvigny ([28, Theorem II]) the following Definition makes sense.

Definition 2.1 *A minimal surface $u(\kappa)$ is called non-degenerate iff rank$D^2\Theta(\kappa) = N$.*

Lemma 2.1 *Non-degenerate minimal surfaces are isolated.*

Proof : Let $u(\kappa)$ be a non-degenerate minimal surfaces, i.e. $\nabla\Theta(\kappa) = 0$, rank$D^2\Theta(\kappa) = N$. By use of the Inverse-function theorem one obtains an open ball $V(\kappa)$ so that $\nabla\Theta(\tilde{\kappa}) \neq 0,\ \tilde{\kappa} \in V(\kappa) \setminus \{\kappa\}$. This proves the Lemma.

In the numerical part of this paper approximations of branches of non-degenerate minimal surfaces will be computed.

3 The discrete approach

Let $\kappa \in T$ and $\alpha \in A$ be fixed. To obtain a conforming finite element method approximating problem (18) first construct a finite dimensional affine space $X_h = X_h(\kappa, \alpha) \subseteq X = X(\kappa, \alpha)$. For this purpose denote by $\tau = \tau(\kappa)$ triangulations of B that are obtained by one of the following refinement strategies.
S1 :(see Fig. 1)

1. (a) $\tau_0 := \cup_{j=1}^{N+3}\Delta(0, e^{i\kappa_{j-1}}, e^{i\kappa_j})$ $(\kappa_0 \equiv \kappa_{N+3} - 2\pi)$ (macro-triangulation)
   (b) Mark the edge $[e^{i\kappa_{j-1}}, e^{i\kappa_j}]$, called refinement edge, of the triangle $\Delta(0, e^{i\kappa_{j-1}}, e^{i\kappa_j})$ $(j = 1, \ldots, N+3;\ \kappa_0 \equiv \kappa_{N+3} - 2\pi)$
   (c) $l = 0$
2. Bisect each $\Delta \in \tau_l$ along the refinement edge. Project new nodes V that belong to the discrete boundary onto ∂B, i.e. set $V = \frac{V}{|V|}$.
3. $l = l + 1$, denote the new set of triangles with τ_l
4. If $l = 2k$ then stop
5. Goto 2.

S2 :(see Fig. 2)

1. (a) $\tau_0 := \cup_{j=1}^{N+3}\Delta(0, e^{i\kappa_{j-1}}, e^{i\kappa_j})$ (macro-triangulation)
   (b) $l = 0$
2. Divide each $\Delta \in \tau_l$ into 4 congruent triangles. Project new nodes V that belong to the discrete boundary onto ∂B, i.e. set $V = \frac{V}{|V|}$.
3. $l = l + 1$, denote the new set of triangles with τ_l
4. If $l = k$ then stop
5. Goto 2.

Clearly, both refinement strategies yield regular and conforming triangulations of B such that the points $\beta_1, \ldots \beta_{N+3}$ are vertices of the final triangulation.

Set

$$B_h := \cup\{\Delta \in \tau\}, \tag{38}$$

$$Y_h := \{v \in C^0(\overline{B}_h, \mathbb{R}^q)\ ; v_{|_\Delta} \text{ linear } \forall\ \Delta \in \tau\}, \tag{39}$$

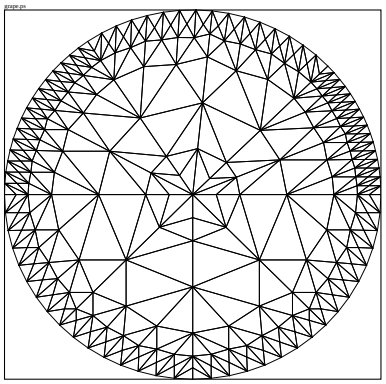

Figure 1: Refinement by bisection

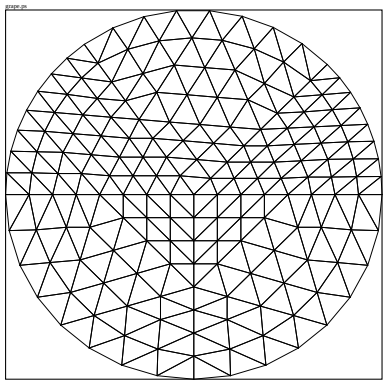

Figure 2: Congruent refinement

and consider Y_h as a subspace of $H^1(B_h, \mathbb{R}^q)$. The discrete analogues of X and X_0 are

$$X_h(\kappa,\alpha) \ := \{v \in Y_h \ ; v(\overline{\gamma}_k(/k) \cap \partial B_h) \subset a_k + \Gamma_k(\alpha) \ (1 \le k \le N+3)\} \tag{40}$$

and

$$X_{h0}(\kappa,\alpha) \ := \ \{v \in Y_h \ ; v(\overline{\gamma}_k(\kappa) \cap \partial B_h) \subset \Gamma_k(\alpha) \ (1 \le k \le N+3)\}, \tag{41}$$

respectively. For functions in Y_h define the discrete Dirichlet integral by

$$D_h(v) := \frac{1}{2}\int_{B_h} |\nabla v|^2 dx. \tag{42}$$

The inclusion $X_h \subseteq X$ can be obtained by use of a suitable prolongation operator for functions in Y_h (see [14]).

The discrete analogue to the variational problem (18) is

$$\Theta_h(\kappa,\alpha) \ = \ \inf_{v \in X_h(\kappa,\alpha)} D_h(v). \tag{43}$$

This problem has a unique solution $u_h = u_h(\kappa,\alpha) \in X_h$, called *discrete quasiminimal surface* that satisfies (see [14, Lemma 4.1])

$$\int_{B_h} \nabla u_h \nabla v \ dx \ = \ 0 \qquad \forall \ v \in X_{h0}. \tag{44}$$

An approximation of $\nabla\Theta_\kappa(\kappa,\alpha)$ is given by

$$f_h^k(\kappa) := -\frac{1}{2}\Big(\frac{1}{\kappa_{k+1}-\kappa_k}\int\limits_{S_h(\kappa_k,\kappa_{k+1})} (u_{h\,x_1}^2(\kappa,\alpha) - u_{h\,x_2}^2(\kappa,\alpha))a(x) + 4u_{h\,x_1}(\kappa,\alpha)u_{h\,x_2}(\kappa,\alpha)b(x)dx_1dx_2 - \tag{45}$$

$$\frac{1}{\kappa_k-\kappa_{k-1}}\int\limits_{S_h(\kappa_{k-1},\kappa_k)} (u_{h\,x_1}^2(\kappa,\alpha) - u_{h\,x_2}^2(\kappa,\alpha))a(x) + 4u_{h\,x_1}(\kappa,\alpha)u_{h\,x_2}(\kappa,\alpha)b(x)dx_1dx_2\Big) \ (k = 1,\dots,N).$$

Concerning the approximation properties of u_h, Θ_h and f_h the following results are proved in [15], [16].

Theorem 3.1 *Let $T' \subset\subset T$, $A' \subset\subset A$ and let $h > 0$ denote the gridsize of a triangulation $\tau_h(\kappa)$ of the unit disc obtained by applying one of the refinement strategies* **S1** *or* **S2**, *respectively. Let u_h, u denote the unique solutions of (43) and (18), respectively. Then one has*

$$\sup_{\kappa \in T', \alpha \in A'} \|u(\kappa,\alpha) - u_h(\kappa,\alpha)\|_{1,B_h} \ \le \ c\ h^{\frac{p-2}{p}} \quad \forall\ 2 \le p < -\frac{2}{p_{min}} \tag{46}$$

with some constant $c = c(T', A') > 0$ and $p_{min} = \inf_{\alpha \in A'} p_{min}(\alpha) > -1$.

Theorem 3.2 *Let Θ and Θ_h denote the functions defined in (18) and (43), respectively. Furthermore let $T' \subset\subset T$ and $A' \subset\subset A$. Then a positive constant $c = c(T', A')$ and some number $p_{min} = p_{min}(A') > -1$ exist so that*

$$\|\Theta - \Theta_h\|_{\infty, T' \times \tilde{A}} \leq c h^{2\frac{p-2}{p}} \quad \forall\ 2 \leq p < \frac{-2}{p_{min}} \tag{47}$$

and

$$\|\nabla_\kappa \Theta - f_h\|_{\infty, T' \times \tilde{A}} \leq c h^{\frac{p-2}{p}} \quad \forall\ 2 \leq p < \frac{-2}{p_{min}}. \tag{48}$$

Remark 3.1 *Since $p_{min}(\alpha) = \min_{1 \leq k \leq N+3}\{-\alpha_k, \alpha_k - 1\}$, where $\alpha_k \pi$ defined by (28) denotes the outer angle at the vertex a_k of the polygon $\Gamma(\alpha)$ $(1 \leq k \leq N+3)$ there holds a direct relation between the smallest angle of the polygon $\Gamma(\alpha)$ and the order of convergence.*

By virtue of eq. (48) it makes sense to define

Definition 3.1 *Let $\kappa \in T$ satisfy $f_h(\kappa) = 0$. The corresponding quasiminimal surface $u_h(k)$ is called discrete minimal surface.*

In [16, Theorem 4.2, Theorem 4.3, Corollary 4.1] existence an convergence of discrete minimal surfaces in neighbourhoods of non-degenerate minimal surfaces is proved. This results can be extended slightly by combining them with the Theorems 3.2, 3.1. For this purpose let $\kappa^* \in T$ be a regular critical point of Θ, i.e.*rank* $D^2\Theta(\kappa^*) = N$ and let $\alpha^* \in A$. The implicit-function theorem now gives the existence of balls $V(\alpha^*) \subset A$, $V(\kappa^*) \subset T$ and an analytic function $\kappa : V(\alpha^*) \to V(\kappa^*)$ such that $\nabla_\kappa \Theta(\kappa^*(\alpha), \alpha^*) = 0$ $\forall \alpha \in V(\alpha^*)$. A set $\{(\kappa^*(\alpha), \alpha); \alpha \in V(\alpha^*)\}$ is called regluar solution branch.

Theorem 3.3 *Let $(\kappa^*(\alpha), \alpha) \in T \times A$ be a regular solution branch. Then for every α there exists a ball $V(\kappa^*(\alpha)) \subset T$ and some $h_0 > 0$ so that for all $0 < h \leq h_0$ the equation*

$$f_h(\kappa, \alpha) = 0$$

has at least one solution $\kappa_h^* = \kappa_h^*(\alpha) \in V(\kappa^*(\alpha))$. For $\alpha \in A' \subset\subset A$ there holds

$$\sup_{\alpha \in A'} |\kappa_h^*(\alpha) - \kappa^*(\alpha)| \leq c\ h^{\frac{p-2}{p}} \quad \forall\ 2 \leq p < \frac{-2}{p_{min}}, \tag{49}$$

$$\sup_{\alpha \in A'} \|u(\kappa^*(\alpha)) - u_h(\kappa_h^*(\alpha))\|_{1, B_h} \leq c h^{(\frac{p}{p-2})^2} \quad \forall\ 2 \leq p < \frac{-2}{p_{min}} \tag{50}$$

and

$$\sup_{\alpha \in A'} |D(u(\kappa^*(\alpha))) - D_h(u_h(\kappa_h^*(\alpha)))| \leq c\ h^{2\frac{p-2}{p}} \quad \forall\ 2 \leq p < \frac{-2}{p_{min}} \tag{51}$$

The constant $c = c(A')$ is positive and $p_{min} = p_{min}(A') > -1$.

Using Corollary 2.1 the proof of this Theorem is a direct consequence of the proof of Theorem 7 and Corollary 3 in [16].

Remark 3.2 *Investigating the question of uniqueness of κ_h^* in Theorem 3.3 would require a deeper analysis of the functions f_h and Df_h (compare [24, Theorem 2]).*

4 Numerical bifurcation of minimal surfaces

In this section numerical investigations on bifurcation of generalized polygonal minimal surfaces are presented. The starting point for further investigations is the vector function $\nabla_\kappa \Theta(\kappa, \alpha)$. According to Theorem 2.2 minimal surfaces $u(\kappa^*, \alpha^*)$ (with Shiffman boundary conditions) that are bounded by the polygon $\Gamma(\alpha^*)$ are characterized by the equation

$$\nabla_\kappa \Theta(\kappa^*, \alpha^*) \;=\; 0.$$

If $\kappa^* \in T$ is a regular critical point of the function Θ, the implicit function theorem implies the existence of a neighbourhood $U(\alpha^*)$ and a function $\kappa^*(\alpha)$ such that

$$\nabla_\kappa \Theta(\kappa^*(\alpha), \alpha) \;=\; 0 \quad (\alpha \in U(\alpha^*)).$$

In this context it might be of interest to examine the structure of the solution set

$$\{(\kappa(\alpha), \alpha); \nabla_\kappa \Theta(\kappa(\alpha), \alpha) \;=\; 0\} \subset \mathbb{R}^N \times \mathbb{R}^{(N+3)q},$$

α varying in certain subsets of A. In the simplest case α varies in a one-parameter family of values, which is the case under consideration.

In the subsequent sections investigations on three one-parameter families of contours $\Gamma_r,\ r \in I$, where $I \subset \mathbb{R}$ denotes a certain closed interval are presented. In this context Shiffman's function will be denoted by $\Theta(\kappa, r)$.

The first family of contours can be obtained by splitting two opposite sides of a regular tetrahedron of side length one into two segments each and pulling these segments slightly apart to positions where they have the distance $r > 0$ (see Fig. 3). These skew octagons will be denoted by Γ_r. In [22] Nitsche proved that there exists a $r_0 > 0$ such that there are at least three minimal surfaces bounded by Γ_r for $0 < r < r_0$. The exact value of r_0 is not yet known, but in [22, p.10] Nitsche proved the estimate $r_0 \leq 0.162733$. Using numerical pathfollowing one is able to improve this estimate experimentally (see Table 2).

The contours in the second one-parameter family of contours are polygonal approximations of the one-parameter family of Enneper contours

$$E_r(\varphi) \;=\; \begin{cases} rcos\varphi \;-\frac{1}{3}r^3 cos3\varphi \\ -rsin\varphi - \frac{1}{3}r^3 sin3\varphi \qquad \varphi \in [0, 2\pi] \\ r^2 cos2\varphi. \end{cases} \tag{52}$$

Several authors investigated the family of Enneper contours and the corresponding minimal surface problem. Parts of these investigations were summarized in the famous book of Nitsche [21] who himself contributed essential steps to the question of uniqueness and non-uniqueness for the family of contours in question. With the help of his famous 4π-theorem, Nitsche proved that there exists a unique minimal surface bounded by E_r for $0 < r < 0,88$ ([21, §A14]). Nitsche also proved that there are at least three minimal surfaces bounded by E_r for $1.68 < r < \sqrt{3}$ ([21, §395]).
In [25] Ruchert proved uniqueness for the Plateau for E_r in the interval $0 < r \leq 1$.
In 1986, Beeson and Tromba rigorously investigated the branching process at $r = 1$ ([1]) and proved that there exists a $r_0 > 1$ such that E_r bounds exactly three minimal surfaces for $1 < r < r_0$ ([1, Corollary 4.4]). Moreover, they were able to characterize the branching process to be of cusp-type (see also [2, Satz 5] where Büch characterized bifurcation of minimal surfaces for two-parameter families of contours based on the Weierstrass representation formula for minimal surfaces).

The third example-contour was suggested by Douglas and Wiener in order to prove non-uniqueness results for the Plateau problem of disc-type surfaces ([5]). A detailed description can be found in Courant's book [3,

p. 120]. In this example the distance between the parallel circles serves as a parameter. In the bifurcation diagrams the $x-axis$ corresponds to the continuation parameter r, the value on the $y-axis$ represents $\kappa(r)^2$.

For families of contours in question solution branches $(\kappa(r), r)$ of the equation

$$f_h(\kappa(r), r) \;=\; 0 \tag{53}$$

are sought numerically. In numerical practice triangulations of the unit disc which are of polar-coordinate type with small grid sizes near the boundary ∂B only are used. In order to obtain smooth discrete surfaces local refinement is applied at the origin (for an example see Fig. 7). Several numerical experiments underlined this choice of grids. Furthermore, for numerical purposes the three-point condition (13) is replaced by a one-point condition, i.e. the parameters $\kappa_{N+1}, \kappa_{N+2}$ are introduced as independant variables. This corresponds to the numerical approximation of the function $\Upsilon(\kappa, 2\pi; \alpha)$.
So far, this was the first time that bifurcation of minimal surfaces was investigated numerically. The main tool in the numerical computations is the ALCON2 SUBROUTINE developed at the Konrad-Zuse Zentrum in Berlin for the purpose of numerical pathfollowing and the detection of simple bifurcation points in the context of one-parameter families of nonlinear equations (for more details see [4]).

4.1 The Lévy - Nitsche example

Let Γ_r $(-2 \le r \le 2)$ denote the set of octagons which are obtained by splitting a regular tetrahedron as described in Section 5.4 (see Fig. 3). Then $\{\Gamma_r\}_r$ is a one-parameter family of closed polygons in $\mathbb{R}^3$. Since for $1 < r \le 2$ the geodesic curvature of Γ_r is less than 4π the polygon Γ_r in this case bounds exactly one solution of Plateau's problem ([27, Eindeutigkeitssatz]). According to [26, Satz 3] $D^2_\kappa \Theta(\kappa(r), r)$ is positive definite and Lemma 2.1 implies the existence of an isolated branch $(\kappa(r), r)$ $(r \in (1, 2]$ such that

$$\nabla_\kappa \Theta(\kappa(r), r) = 0.$$

For $h > 0$ sufficiently small Theorem 3.3 now yields the existence of a numerical branch $(\kappa_h(r), r)$ such that

$$f_h(\kappa_h(r), r) = 0$$

and there is hope that pathfollowing started with $r \in (1, 2]$ leads to distinct solution branches for $r \in (0, 1)$ each representing distinct discrete minimal surfaces spanning Γ_r.

In the following the numerical results that are obtained by applying the ALCON2 program are presented.

Table 1 shows the numerical data for the grids in use. For the refinement levels (RL) one, two and three no numerical bifurcation was detected. In this cases one obtaines a unique numerical branch

$$\{(\kappa_h(r), r); f_h(\kappa_h(r), r) = 0,\ r \in [-2, 2]\}.$$

Numerical bifurcation is reported for $RL \ge 4$. The corresponding bifurcation intervals are presented in Table 2. The ALCON2 program computes three solution branches $(\kappa^1(r), r), (\kappa^2(r), r), (\kappa^3(r), r)$ such that

$$f_h(\kappa^i(r), r) \;=\; 0 \qquad i = 1, 2, 3 \quad (r_0 < r < r_1).$$

In order to decide whether these three branches represent stable or unstable discrete minimal surfaces the eigenvalues of some finite-difference approximation $D_\epsilon f_h(\kappa^i(r), r)$ $(i = 1, 2, 3)$ of Df_h at some parameter values $r \in (r_0, r_1)$ are computed. It turned out that two branches $(\kappa^i(r), r)$ $(i = 1, 3)$ represent stable branches, i.e all eigenvalues of $D_\epsilon f_h(\kappa^i(r), r)$ $(i = 1, 3)$ are positive and the branch $(\kappa^2(r), r)$ represents unstable discrete minimal surfaces, i.e. $D_\epsilon f_h(\kappa^2(r), r)$ posseses one negative eigenvalue.

RL	*triangles*	*nodes*	*boundary nodes*
1	352	209	64
2	800	465	128
3	1696	977	256
4	3488	2001	512
5	7072	4049	1024
6	14240	8145	2048

Table 1: Correspondence between RL and triangles, nodes and boundary nodes

At the bifurcation points $N+1$ eigenvalues of $D_\epsilon f_h(\kappa(r_i), r_i)$ $(i = 0, 1)$ are positive and one eigenvalue has the size $5.e-5 < tol$, where $tol = 1.e-3$ was the required computational accuracy.

At the intervals $[-2, r_0)$ and $(r_1, 2]$ a single numerical branch that represents stable discrete minimal surfaces is reported. In Figs. 4, ..., 6 the bifurcation diagrams for the refinement levels four, five and

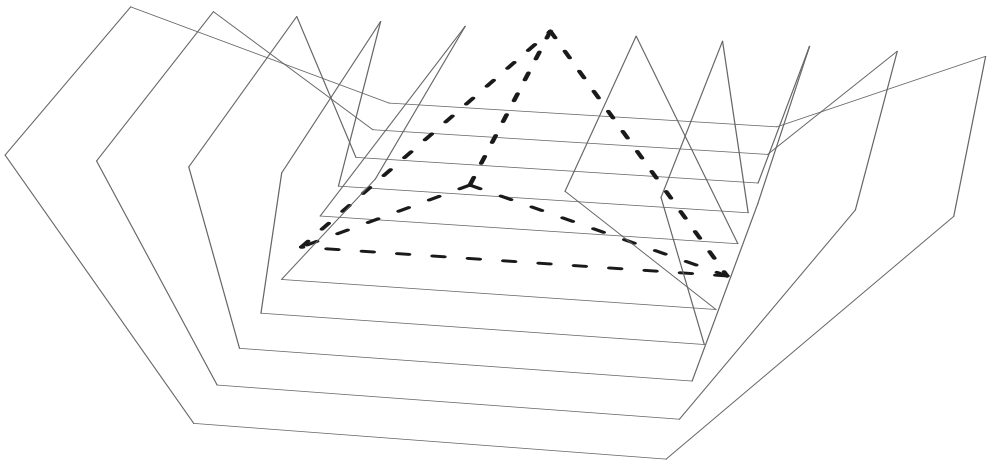

Figure 3: Contour family Γ_r

six, respectively are presented. Figs. 7, ..., 12 show three discrete minimal surfaces together with their triangulations for $RL = 4$ at $r = 0.24$. Dirichlet's integral for the surface in Fig. 8 has the value 1.3667, while the discrete area equals 1.2994. For the surfaces in Fig. 10 and Fig. 12 both energies have the value 1.3613, the discrete area of both surfaces is 1.2616.

Nitsche investigated the family of contours in question in [22], where he proved the existence of at least three minimal surfaces bounded by Γ_r for $r \in (0, 0.162733)$. Therefore these numerical experiments improve the size of Nitsches interval of non-uniqueness experimentally.

RL	r_0	r_1
1	-	-
2	-	-
3	-	-
4	-0.194634	0.425498
5	-0.345394	0.485104
6	-0.460096	0.512496

Table 2: Bifurcation in dependence to fineness

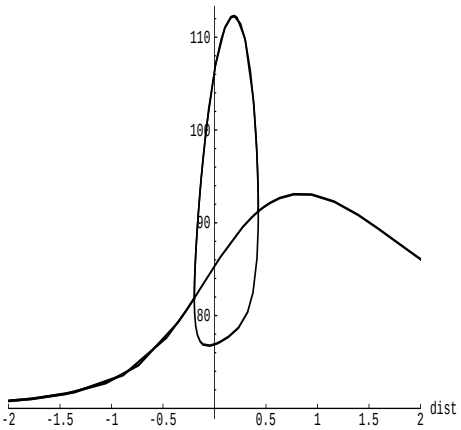

Figure 4: Bifurcation diagram, RL 4

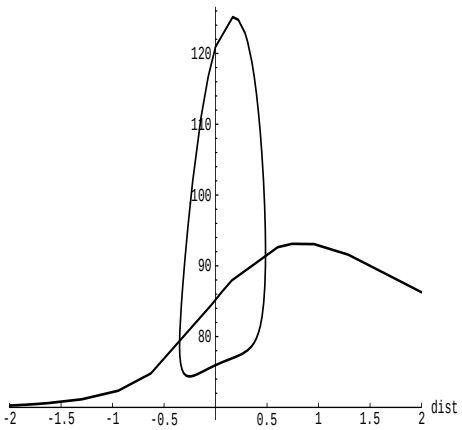

Figure 5: Bifurcation diagram, RL 5

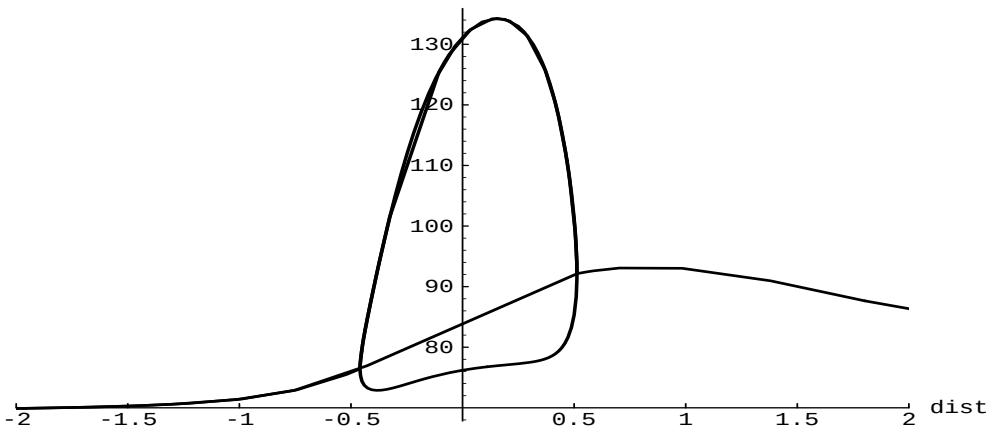

Figure 6: Bifurcation diagram, RL 6

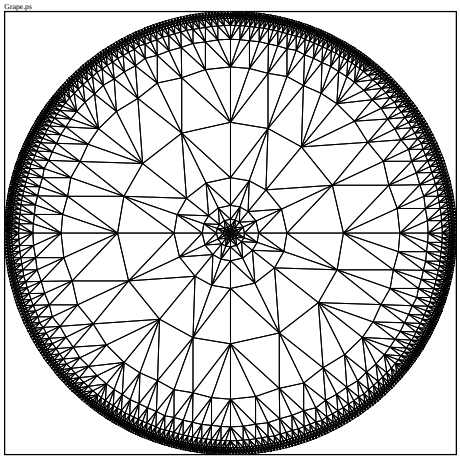

Figure 7: Triangulation, RL 4 , r = 0.24, branch 1

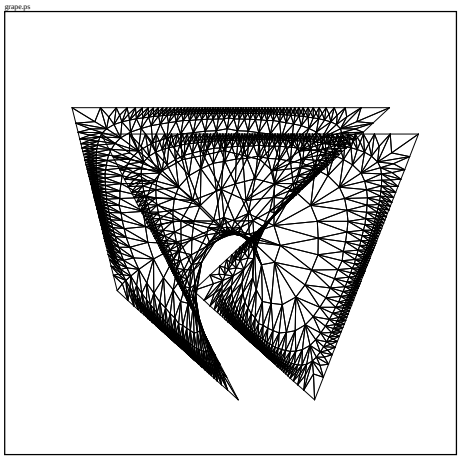

Figure 8: Corresponding minimal surface, branch 1, r = 0.24

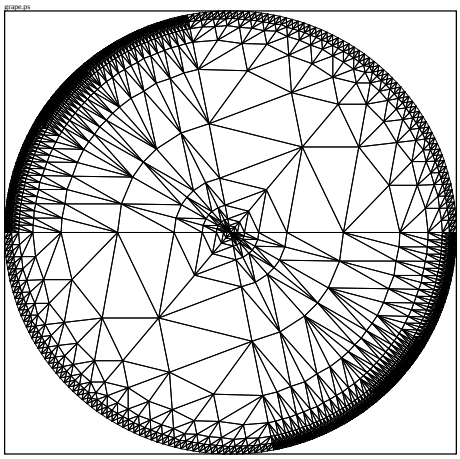

Figure 9: Triangulation, RL 4 , r = 0.24, branch 2

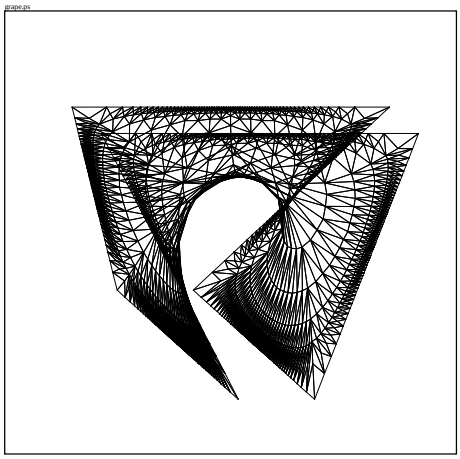

Figure 10: Corresponding minimal surface, branch2, r = 0.24

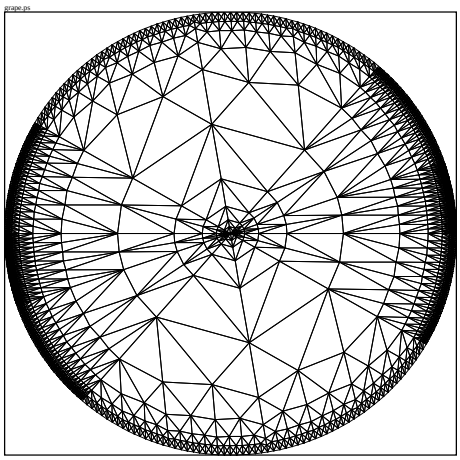

Figure 11: Triangulation, RL 4 , r = 0.24, branch 3

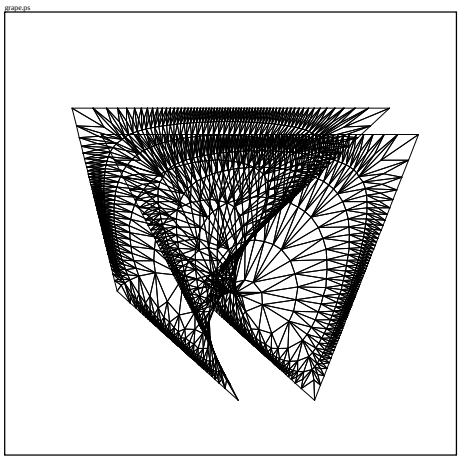

Figure 12: Corresponding minimal surface, branch3, r = 0.24

4.2 Polygonal approximations of Enneper's contour

In the present section some numerical investigations concerning the branching of discrete minimal surfaces that are bounded by polygonal approximations of Enneper's contour (52) are presented. Polygonal approximation of Enneper's contour can be obtained as follows. For $n \in \mathbb{N},\ n \geq 4$ subdivide the interval $[0, 2\pi]$ into n parts

$$[0, \varphi_1], [\varphi_1, \varphi_2], \ldots, [\varphi_{n-1}, 2\pi],$$

where

$$\varphi_i \ := \ 2\pi \frac{i}{n} \qquad 0 \leq i \leq n-1.$$

The polygon Γ_n^r then is defined by the $n =: N+3$ vertices $a_i := E_r(\varphi_i)\ (0 \leq i \leq n-1)$.

The numerical results in this section are obtained by applying the ALCON2 program to the equation

$$f_h(\kappa, r) = 0 \quad (\kappa \in Q,\ r \in [0.1, 8])$$

The cases $n = 12$ and $n = 18$ are considered.

Table 3 shows the numerical data for the triangulations that are used. For refinement level (RL) one an unique numerical branch

$$\{(\kappa(r), r);\ f_h(\kappa(r), r) = 0,\ r \in [0.1, 8]\}$$

is reported by the ALCON2 routine in both of the cases $n = 12$ and $n = 18$.

For $RL \geq 2$ the ALCON2 program was not able to resolve the solution set of the equation $f_h(\kappa, r) = 0$ completely. At the parameters r_0, that are presented in the Tables 4, 5 ALCON2 terminated, since the steplength in the pathfollowing algorithm became too small. But ALCON2 also reported a turning point as well as a bifurcation point at r_0. This fact indicated that the bifurcation process at r_0 might not be simple and therefore might be identified to be of $cusp - type$ (compare [2, Bild1]). For the definition of turning points and simple bifurcation points we refer to [4, (2.0.1),(2.0.2)].

The bifurcation diagrams in the present section are obtained by applying pathfollowing to the equation

$$f_h(\bar{\kappa}, \kappa^*_{N+2}, r) = 0,$$

where κ^*_{N+2} is kept fixed. The ALCON2 program computes a single solution path $(\bar{\kappa}(r), r)$ (see Fig. 13). Then choose some parameter $r^* > r_0$ and use a damped Gauss - Newton technique to fit the fixed variable κ^*_{N+2} at the parameter value r^*. In this way one obtaines some $(\kappa(r^*), r^*)$ such that $f_h(\kappa(r^*), r^*) = 0$. Then start the ALCON2 program in the single-path following mode at $r = r^*$. In the single-path following mode the ALCON2 program indicates whether singular points lying on the solution path are crossed, but suppresses their computation.

4.2.1 Polygonal approximation with 12 vertices

In the case $n = 12$ Γ_r^n according to Sauvigny's uniqueness theorem [27, Eindeutigkeitssatz] bounds a unique minimal surfaces for $r \in (0, 0.970862)$. Therefore, one could expect that there exist an isolated solution branch $(\kappa(r), r)$ such that $f_h(\kappa(r), r) = 0$ $(r \in (0, 0.970862))$. Starting the pathfollowing algorithm at $r = 0.1$ one obtains a unique numerical branch for $RL = 1$. For $RL \geq 2$ the situations changed and numerical bifurcation in the interval (r_0, r_1) is observed. In contrast to the Lévy - Nitsche example increasing the number of refinement levels yielded bifurcation intervals (r_0, r_1) where only r_0 seems to be bounded from below and the value of r_1 becomes greater in proportion to decreasing gridsize. In Figs. 14, 15, 16 and 17 the

RL	$n = 12$	nt	nn	nb	$n = 18$	nt	nn	nb
1		528	313	96		792	469	144
2		1200	697	192		1800	1045	288
3		2544	1465	384		3816	2197	576
4		5232	3001	768		7560	4357	1152
5		10608	6073	1536		15552	8929	2304

Table 3: RL in correspondence to triangulation data

RL	r_0	r_1
1	-	-
2	1.31962	3.17112
3	1.22335	4.67198
4	1.19285	6.19521
5	1.18187	7.65548

Table 4: Bifurcation in dependence to gridsize, n=12

bifurcation diagrams corresponding to $RL = 2, 3, 4, 5$ are shown. As in Section 4.1 three solution branches $(\kappa^i(r), r)$ $(i = 1, 2, 3)$ are reported such that

$$f_h(\kappa^i(r), r) = 0 \quad (r \in (r_0, r_1)).$$

Two branches represent stable discrete minimal surfaces and one solution path represents unstable discrete minimal surfaces. In the intervals $[0.1, r_0]$ and $[r_1, 8]$ a unique stable numerical branch is obtained.

At the bifurcation parameters r_0, r_1 $N + 1$ eigenvalues of the matrices $D_\epsilon f_h(\kappa(r^i), r^i)$ $(i = 0, 1)$ are positive and one eigenvalue is smaller than the prescribed computational accuray $tol = 1.e - 3$.

As Fig. 17 shows, the ALCON2 program also computed two turning points in a neighbourhood of r_1. This might be caused by numerical reasons. On the other hand this fact might indicate that Enneper's contour bounds more than three minimal surfaces for certain parameter values r.

Selected discrete minimal surfaces together with the corresponding grids are presented in Figs. 18, ..., 23 for the parameter value $r = 1.25$ and $RL = 4$. The energy of the surface in Fig. 19 is 13.773, the discrete area has the value 13.68. Dirichlet's integral for the surfaces in Figs. 21 and 23 is 13.75, the discrete area of both surfaces is 13.563. As an orientation we also computed the surface area

$$S(r) \;=\; \pi\, r^2(1 + r^2 + \frac{1}{3}r^4)$$

of Enneper's surface. We obtained $S(1.25) = 16.57$. The matrix $D_\epsilon f_h(\kappa^1(1.25), 1.25)$ has one negative eigenvalue, the matrices $D_\epsilon f_h(\kappa^i(1.25), 1.25)$ $(i = 2, 3)$ are positive definite. Therefore these three discrete surfaces might be approximations of two local minima and an unstable critical point of the area functional.

4.2.2 Approximation with 18 vertices

The case $n = 18$ is treated in the same way as the case $n = 12$, excepted that for $RL = 4, 5$ triangulations with small gridsize near the boundary ∂B of B only (see Fig. 34) are used. For $RL = 1, 2, 3$ bifurcation

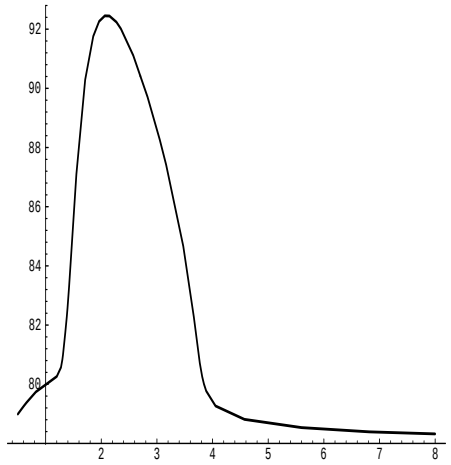

Figure 13: Bifurcation diagram, κ_{N+2} fixed, RL 2, $n = 12$

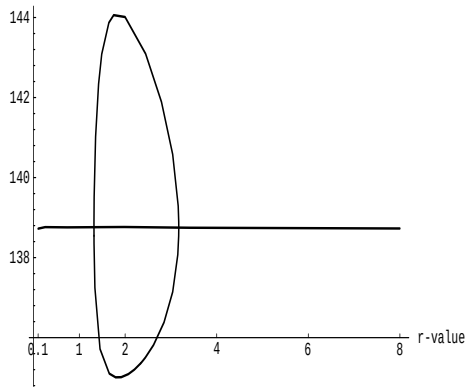

Figure 14: Bifurcation diagram, RL 2, $n = 12$

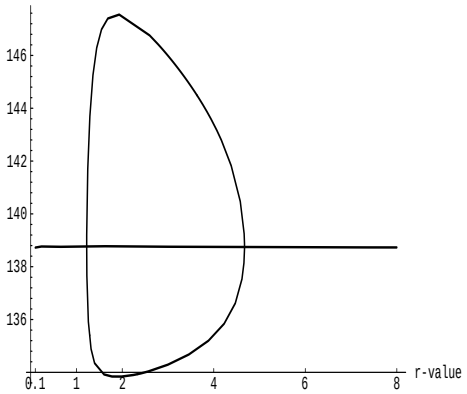

Figure 15: Bifurcation diagram, RL 3, $n = 12$

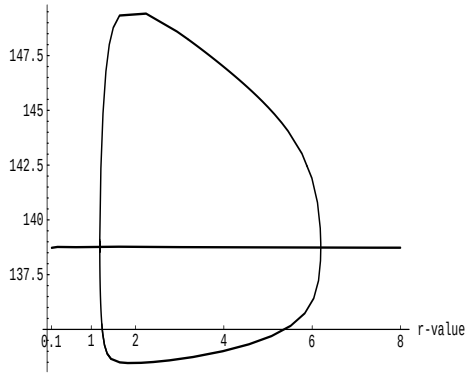

Figure 16: Bifurcation diagram, RL 4, $n = 12$

diagrams similar to that in the case $n = 12$ are computed by the ALCON2 program. Again one observes that r_0 seems to be bounded from below and r_1 becomes greater in proportion to the gridsize of the corresponding triangulations (compare Figs. 24, 25). Table 5 shows the bifurcation intervals corresponding the the different refinement levels. In Figs. 24 and 25 we present two bifurcation diagrams corresponding to $RL = 2, 3$. Figs. 26, ..., 31 show selected minimal surfaces together with the corresponding triangulations at $r = 1.2$ for $RL = 3$. The energy of the surface in Fig. 27 is 13.1547, the discrete area has the value 13.0797. Enneper's surface has the area $S(1.2) = 14.1652$. The surfaces in Figs. 29 , 31 both have the area 12.9218, their energy has the value 13.1128. The matrix $D_\epsilon f_h(\kappa^1(1.2), 1.2)$ has one negative eigenvalue, the matrices $D_\epsilon f_h(\kappa^i(1.2), 1.2)$ $(i = 2, 3)$ are positive definite. Therefore, these three discrete minimal surfaces might be approximations of two local minima and an unstable critical point of the area functional.

Figs. 32 and 33 show bifurcation diagrams for $RL = 4, 5$. As one can see, the three different branches become nearly parallel for $r > r_0$. Moreover, the solution branches are no longer convex curves. This fact might indicate that Enneper's contour E_r bounds more than three minimal surfaces for some parameter values $r > r_0$.

Figs 34, 35 show the grid together with the discrete minimal surface at $r = 1, 12$ corresponding to a

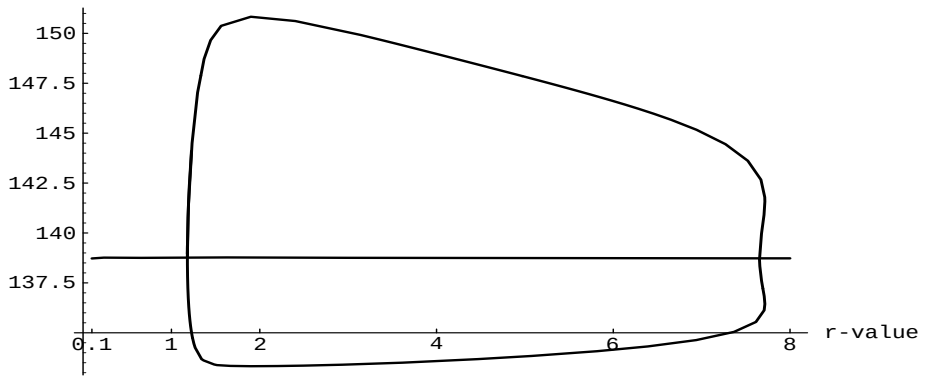

Figure 17: Bifurcation diagram, RL 5, $n = 12$

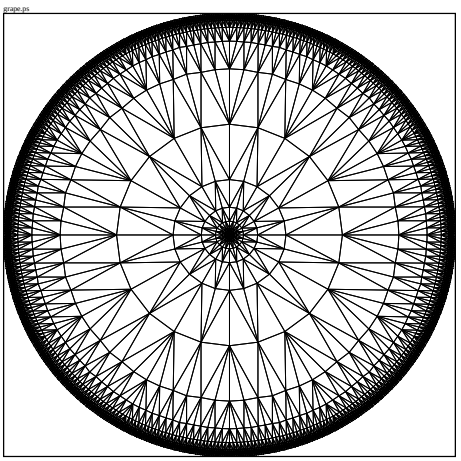

Figure 18: Triangulation, RL4, $r = 1.25$, branch 1

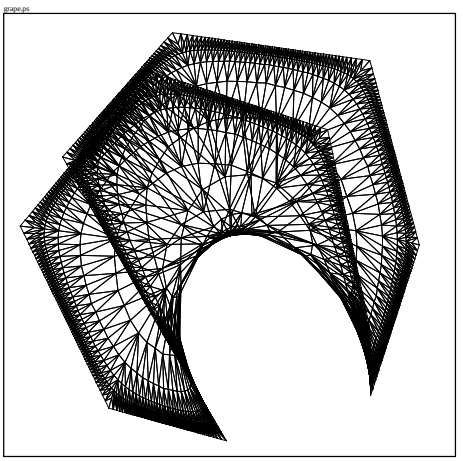

Figure 19: Minimal surface, RL4, $r = 1.25$, branch 1

stable branch for $RL = 4$. The energy of the surface is 10.485, the area of the surface has the value 10.381. The surface area of Enneper's surface is $S(1.12) = 10.952$.

Note that the computational time on an IBM RISC System/6000 for obtaining the bifurcation diagrams that are presented in this section and in Section 4.1 varied between a few minutes (RL 1, 8 vertices) and several days (RL 5, 18 vertices).

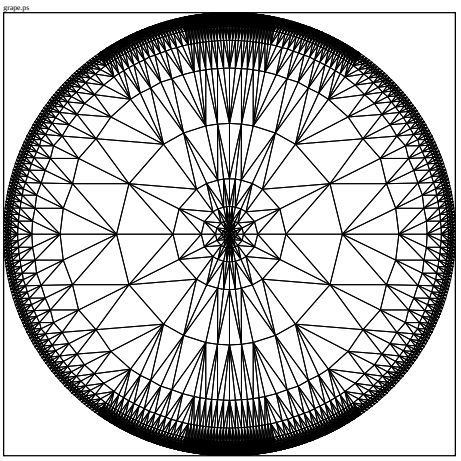

Figure 20: Triangulation, RL4, $r = 1.25$, branch 2

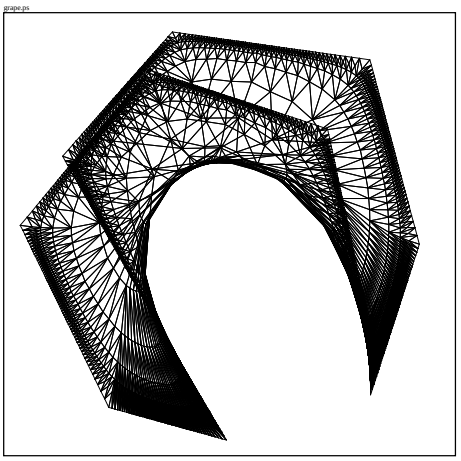

Figure 21: Minimal surface, RL4, $r = 1.25$, branch 2

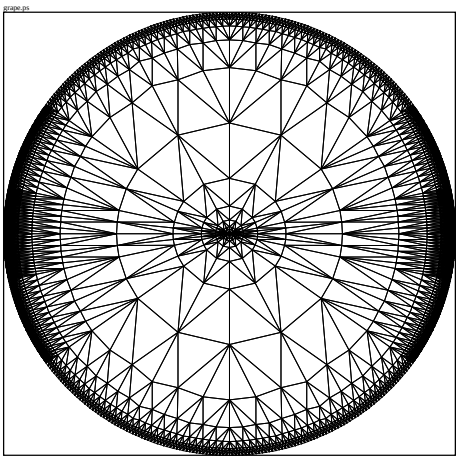

Figure 22: Triangulation, RL4, $r = 1.25$, branch 1

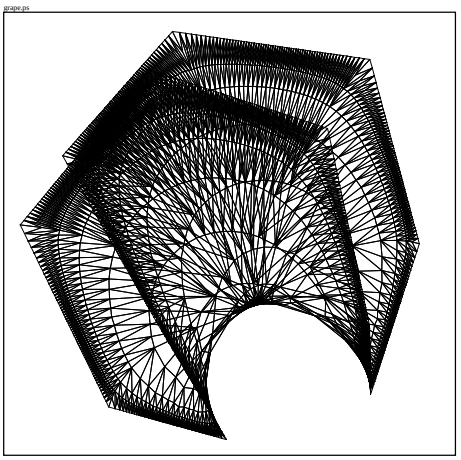

Figure 23: Minimal surface, RL4, $r = 1.25$, branch 1

RL	r_0	r_1
1	-	-
2	1.16277	4.22471
3	1.12154	6.2248
4	1.08284	> 8
5	1.07885	> 8

Table 5: Bifurcation in dependence to fineness, n=18

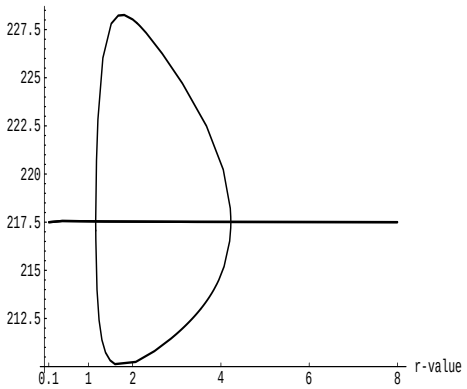

Figure 24: Bifurcation diagram, RL 2, $n = 18$

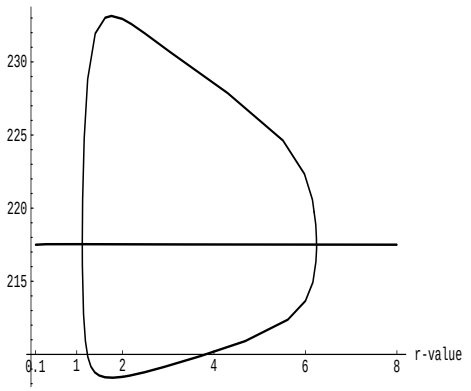

Figure 25: Bifurcation diagram, RL 3, $n = 18$

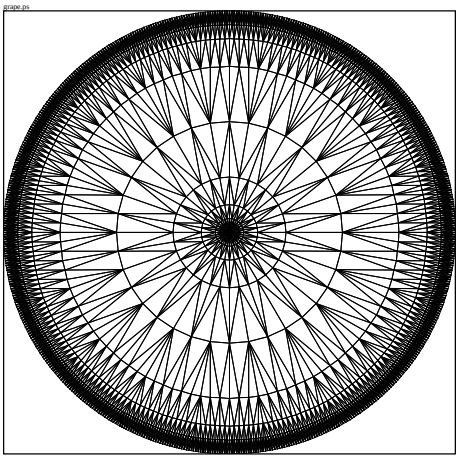

Figure 26: Triangulation, RL 3, $r = 1.2$, branch 1

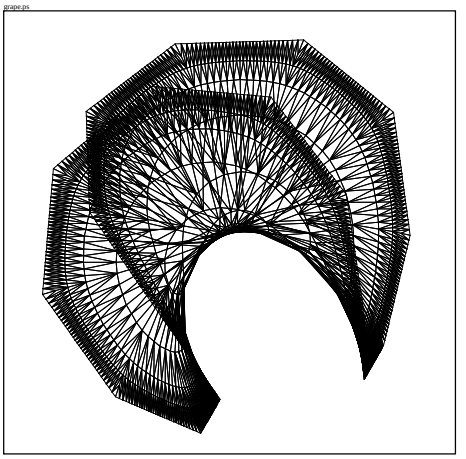

Figure 27: Minimal surface, RL 3, $r = 1.2$, branch 1

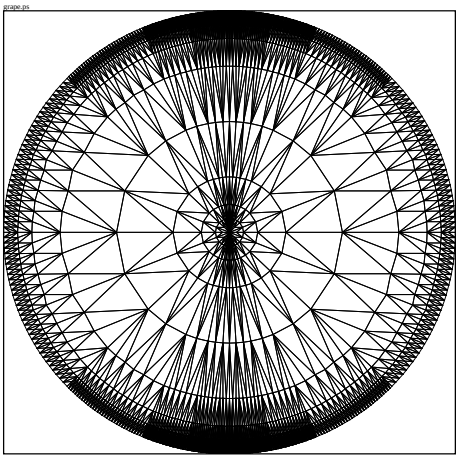

Figure 28: Triangulation, RL 3, $r = 1.2$, branch 2

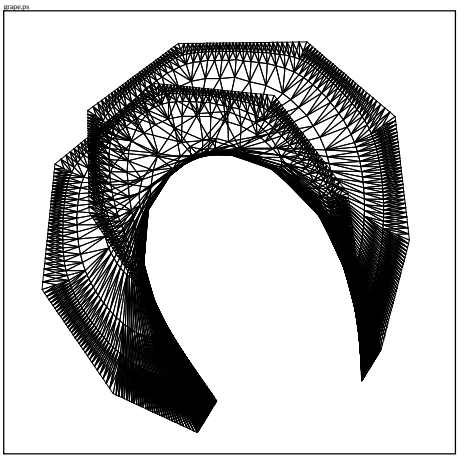

Figure 29: Minimal surface, RL 3, $r = 1.2$, branch 2

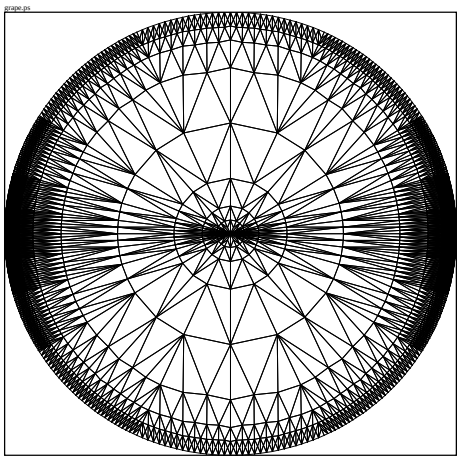

Figure 30: Triangulation, RL 3, $r = 1.2$, branch 3

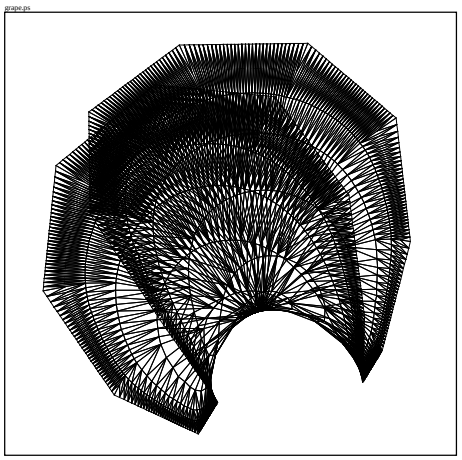

Figure 31: Minimal surface, RL 3, $r = 1.2$, branch 3

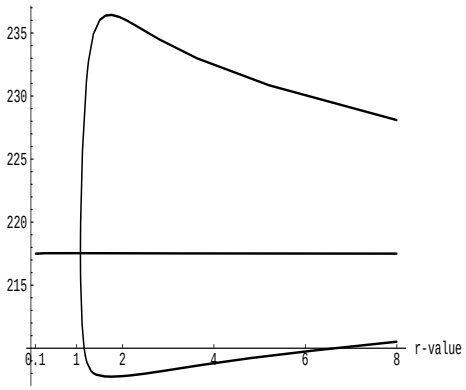

Figure 32: Bifurcation diagram, RL 4, $n = 18$

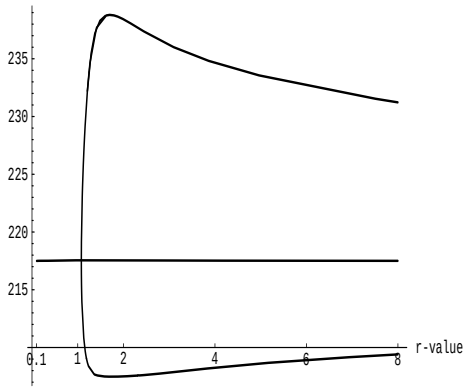

Figure 33: Bifurcation diagram, RL 5, $n = 18$

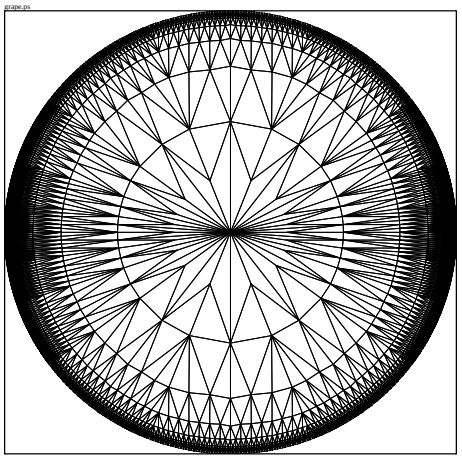

Figure 34: Triangulation RL4, $r = 1, 12$

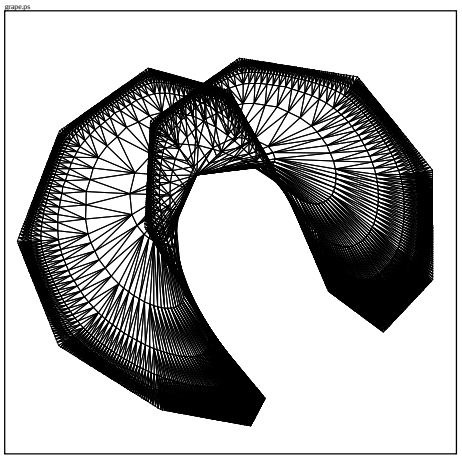

Figure 35: Minimal surface, RL 4, $r = 1, 12$, branch 2

4.3 The Douglas-Wiener-Courant example

In this section the following family of contours is considered. Place two parallel circles of equal radius equal to one perpendicularly to the $z-axis$ at a distance r. Connect the two circles by a strip of width $2\sin\frac{\pi}{20}$ and remove parts of the circles such that the remaining contour becomes a Jordan curve. Denote the equidistant polygonal approximations of these contours by Γ_r. The distance r then serves as a continuation parameter.

Due to results of Courant [3, p.120] for certain parameter values r the contours Γ_r bound at least two minimal surfaces. One of them, the catenoidal surface, furnishes a strong relative minimum of the area-functional. The other minimal surface reported in [3, p.120] has smaller area than the catenoidal surface, but it is not clear whether this surface is in some sense stable, i.e. furnishes a relative minimum of the area-functional.

The numerical investigations presented here indicate that this surface in fact seems to be stable. Furthermore, by a mountain-path argument, there is then another minimal surface spanning Γ_r. As the numerical experiments show this seems to be true.

In the following some numerical investigations for polygonal approximation with 16 vertices are presented. The results for approximations with 20, 24 or 28 vertices are similar and therefore are omitted here.

In contrast to the previous examples no bifurcation at all occurs when applying numerical pathfollowing to the equation

$$f_h(\kappa, r) = 0, \quad r \in [\frac{1}{2}, 2].$$

The numerical experiments always yield a single numerical branch $(\kappa_h(r), r)$ and no turning points are observed up to refinementlevel (RL) 2. For RL $\geq$3 the situation changes. The ALCON2 program computes a single solution branch with 2 turning points at the parameter values r_1 and r_2, say (see Figs. 36, 37). Clearly, for $r \in (r_1, r_2)$ the contour Γ_r bounds at least 3 discrete minimal surfaces and the contours Γ_{r_1} and Γ_{r_2} seem to bound exactly 2 discrete minimal surfaces. The parameter values of the turning points are $r_1 = 1.09, r_2 = 1.2$ for RL=3, $r_1 = 0.96, r_2 = 1.29$ for RL=4. In Figs. 38,...,43 three discrete minimal surfaces together with their triangulations are shown. The suraces in Figs. 39, 43 are stable, i.e. $D_\epsilon f_h(\kappa_h(r), r)$ has positive eigenvalues. The surface areas are 6.72 and 7.01, Dirichlet's integral has the values 7.14 and 7.24. The surface in Fig. 40 is unstable, i.e. $D_\epsilon f_h(\kappa_h(r), r)$ has one negativ eigenvalue. The surface area is 7.14, Dirichlet's integral for the surface has the value 7.27.

In Figs. 44,...,47 discrete minimal surfaces corresponding to the turning point parameters are presented. At the turning points $D_\epsilon f_h(\kappa_h(r_i), r_i),\ i = 1, 2)$ has positive eigenvalues, one eigenvalue always is lower than the prescribed computational accuracy $tol = 10^{-3}$. The surfaces in Figs. 44, 45 have surface areas 5.91 and 5.32. The values of the Dirichlet integral are 6.13 and 5.69. For the surfaces in Figs. 46, 47 one computes the values 7.55 and 7.04 for the area, 7.72 and 7.51 for the energy.

Remark 4.1 *Instead of using the distance r one may introduce the strip-width as a continuation parameter while r chosen suitably in the interval* $[1, 2]$*, say is kept fix. The numerical results in this case are similar.*

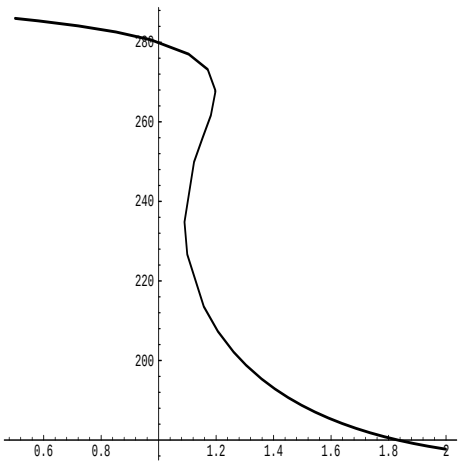

Figure 36: Branch, RL 3

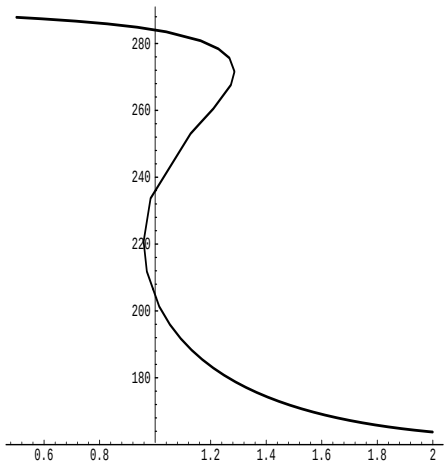

Figure 37: Branch, RL 4

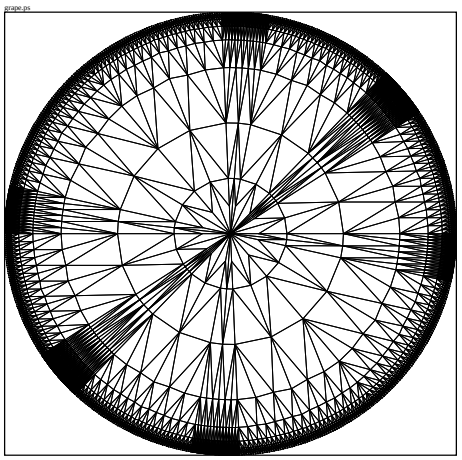

Figure 38: Triangulation 1, RL 4, $r = 1.2$

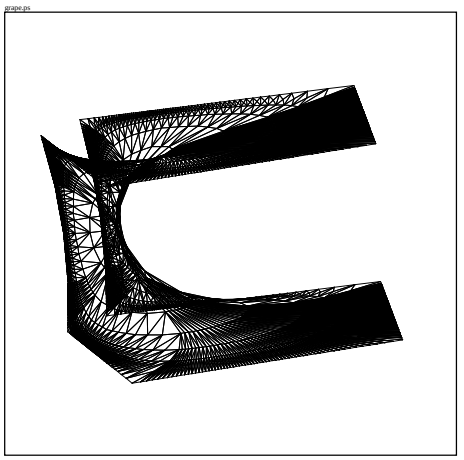

Figure 39: Minimal surface 1, RL 3, $r = 1.2$

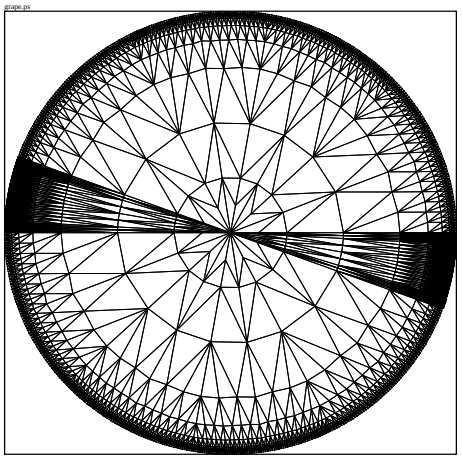

Figure 40: Triangulation 2, RL 4, $r = 1.2$

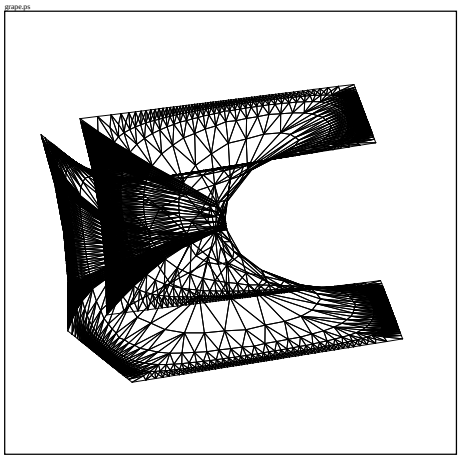

Figure 41: Minimal surface 2, RL 4, $r = 1.2$

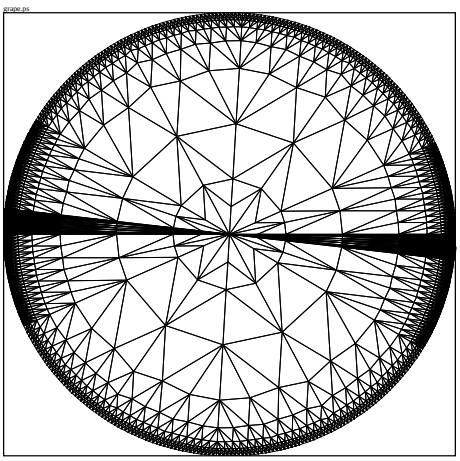

Figure 42: Triangulation 3, RL 4, $r = 1.2$

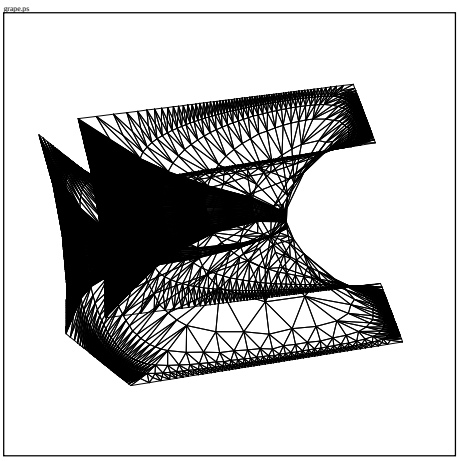

Figure 43: Minimal surface 3, RL 4, $r = 1.2$

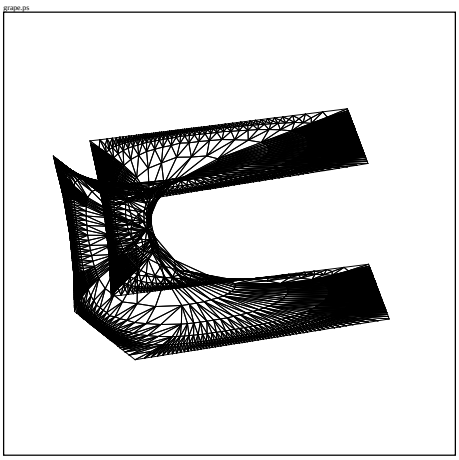

Figure 44: Minimal surface, TP1, $r = 0.96$

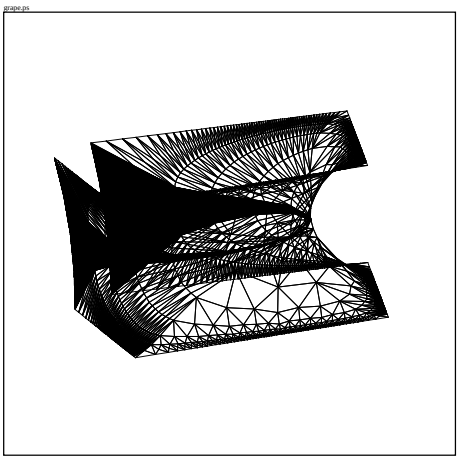

Figure 45: Minimal surface, RL 4, $r = 0.96$

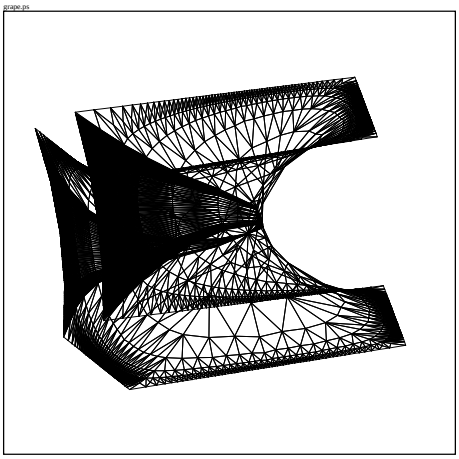

Figure 46: Minimal surface, TP2, $r = 1.29$

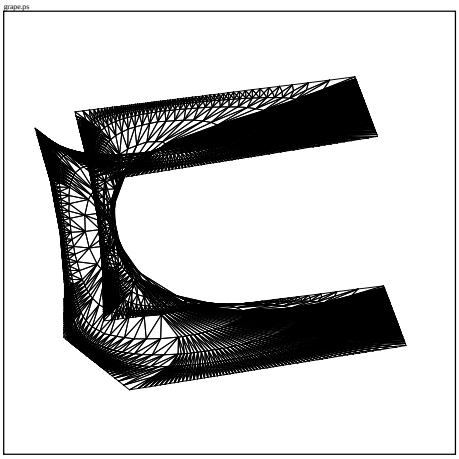

Figure 47: Minimal surface, RL 4, $r = 1.29$

References

[1] M.J. Beeson, A.J. Tromba. The Cusp Catastrophe Of Thom In The Bifurcation Of Minimal Surfaces. man. math. 46, 273-308 (1984)

[2] J. Büch. Bifurkation von Minimalflächen und elementare Katastrophen. man. math. 55, 269-306 (1986)

[3] R. Courant. Dirichlet's Principle. Interscience Publishers 1950

[4] P. Deuflhard, B. Fiedler, P. Kunkel. Efficient Numerical Pathfollowing Beyond Critical Points. Siam J. Numer. Anal. 24, 912-927 (1987)

[5] J. Douglas. Solution of the Problem of Plateau. Trans. Amer. Math. Soc. 33, 263-321 (1931)

[6] G.Dziuk. An Algorithm for Evolutionary Surfaces. Numer. Math. 58, 603-611 (1991)

[7] G.Dziuk, J.E. Hutchinson On The Approximation Of Unstable Parametric Minimal Surfaces. Preprint No. 2o. 340, SfB 256, Universität Bonn, Germany (1994)

[8] E. Heinz. Über die analytische Abhängigkeit eines linearen elliptischen Randwertproblems von Parametern. Nachr. Akad. Wiss. Gottingen, 1-20 (1979)

[9] E. Heinz. Über eine Verallgemeinerung des Plateau'schen Problems. Manuscipta Math. 28, 81-88 (1979)

[10] E. Heinz. Ein mit der Theorie der Minimalflächen zusammenhängendes Variationsproblem. Nachr. Akad. Wiss. Göttingen, 25-35 (1980)

[11] E. Heinz. (1983): Zum Marx-Shiffmanschen Variationsproblem. J. Reine u. Angew. Math. **344**, 196-200

[12] E. Heinz. Minimalflächen mit polygonalem Rand. Math. Z. 183, 547-564 (1983)

[13] M. Hinze. Zur numerischen Behandlung des Marx-Shiffman-Randwertproblems. Diplomarbeit, Institut für Angew. Math., Universtät Bonn, 1989

[14] M. Hinze. On the numerical Treatment of Quasiminimal Surfaces. Impact of Computing in Science and Engineering 5, 249-270 (1993)

[15] M. Hinze. On the Numerical Treatment of Minimal Surfaces with Polygonal Boundaries. Ph.D., Technical University Berlin, Germany (1994)

[16] M. Hinze. On the Numerical Approximation of Unstable Minimal Surfaces with Polygonal Boundaries Num. Math., to appear (1995)

[17] J.E. Hutchinson. Computing Conformal Maps and Minimal Surfaces. Proc. Centr. Math. Anal., Canberra, 26 (1991)

[18] H. Jarausch Zur Numerischen Behandlung Von Parametrischen Minimalflächen Mit Finiten Elementen. Dissertation, Ruhr Universität Bochum, Germany

[19] F. Lewerenz. Eine Bemerkung zu den Marx-Shiffman'schen Minimalvektoren bei Polygonen. Arch. Rat. Mech. Anal. 78 (1981)

[20] I. Marx. On the Classification of Unstable Minimal Surfaces with Polygonal Boundaries. Communications on Pure and Applied Mathematics, Vol. 8, 235-244 (1955)

[21] J.C.C Nitsche. Lectures on Minimal Surfaces Volume 1. Cambridge University Press 1989

[22] J.C.C. Nitsche. Contours Bounding at Least Three Solutions of Plateau's Problem. Arch. Rat. Mech. Anal. 30, 1-11 (1968)

[23] U. Pinkall, K. Polthier Computing Discrete Minimal Surfaces And Their Conjugates. SFB 288 Preprint No. 49, Technical University Berlin, Germany

[24] J. Pousin, J. Rappaz. (1994) Consistency, stability, a priori and a posteriori errors for Petrov-Galerkin methods applied to nonlinear problems. Numer. Math. **69**, 213-231

[25] H. Ruchert. A Uniqueness Result for Enneper's Minimal Surface. Ind. Univ. Math. J. 30, 427-431 (1981)

[26] F. Sauvigny. Die zweite Variation von Minimalflächen im $\mathbb{R}^p$ mit polygonalem Rand. Math. Z. 189, 167-184 (1985)

[27] F. Sauvigny. Ein Eindeutigkeitssatz für Minimalflächen im $\mathbb{R}^p$ mit polygonalem Rand. Journal f. d. Reine und Angew. Math. 358, 92-96 (1985)

[28] F. Sauvigny. On the Morse index of minimal surfaces in $\mathbb{R}^p$ with polygonal boundaries. Manuscripta math. 53, 167-197 (1985)

[29] T. Tsuchija. On Two Methods For Approximating Minimal Surfaces In Parametric Form. Math. Comp. 46, 512-529 (1986)

[30] T. Tsuchija. Discrete Solution of the Plateau Problem and Its Convergence. Math. Comp. 49, 157-165 (1987)

[31] T. Tsuchija. A Note On Discrete Solutions Of the Plateau Problem. Math. Comp. 54, 131-138 (1990)

[32] O. Wohlrab. Zur numerischen Behandlung von parametrischen Minimalflächen mit halbfreien Rändern. Preprint No. 739, SFB 72 Universität Bonn